Journal of Solid Mechanics Vol. 7, No. 4 (2015) pp. 429-441

Analysis of Axisymmetric Extrusion Process through Dies of any Shape with General Shear Boundaries

H. Haghighat [1,*], G.R. Asgari [2]

[1]*Mechanical Engineering Department, Razi University, Kermanshah, Iran*
[2]*Faculty of Mechanical Engineering , Shahid Rajaee Training University, Tehran, Iran*

Received 28 July 2015; accepted 1 October 2015

ABSTRACT

In this paper, a generalized expression for the flow field in axisymmetric extrusion process is suggested to be valid for any dies and the boundary shapes of the plastic deformation zone. The general power terms are derived and the extrusion force is calculated by applying upper bound technique for a streamlined die shape and exponential functions for shear boundaries. It is shown that assuming exponential boundaries for deformation zone yields a die shape with smaller extrusion force than that of by assuming spherical shape boundaries is in agreement with the results obtained by the finite element method.

Keywords : Axisymmetric extrusion; Velocity field ; Upper bound method.

1 INTRODUCTION

AXISYMMETRIC extrusion, round to round, is a plastic deformation process in which a round billet is forced to flow by compression through the die opening of a smaller cross-sectional area than that of the original billet. The pressure required for axisymmetric extrusion is a function of the process parameters (reduction, friction factor, and die shape). For a particular extrusion process, the size of billet, the reduction and the friction factor are constant. The main factor affecting on extrusion process is the die shape. Therefore, the determination of the specific die shape, which meets the minimum extrusion pressure, is important.

Among various approximate methods of solution, upper bound solutions are found by minimizing the total power formulated from a chosen kinematically admissible velocity field. The assumption of velocity field will influence the prediction of extrusion pressure, metal flow and optimized die shape. There is no method available in the literature for constructing kinematically admissible velocity fields appropriate for the problem under consideration. It is always desirable to utilize a velocity field, which is as close to reality as possible. Even though the velocity field may not exactly match the flow behavior of the material, if it is chosen carefully, valuable insight about the process can be obtained. It is often necessary to include extra variables or parameters in the velocity field in order to produce a realistic description of the actual flow. The best value for a variable is the one, which requires the minimum amount of externally supplied power for the process to occur.

Considerable attention has been focused on the upper bound analysis of axisymmetric extrusion through variety of die shapes by assuming appropriate velocity fields. Avitzur [1–4] examined axisymmetric extrusion through conical dies using upper bound model. The boundaries at the entrance and the exit of the deformation zone, which are also shear surfaces or velocity discontinuity surfaces, have been assumed by Avitzur as two concentric spherical surfaces with their centre at the virtual apex of the cone of the die. Zimerman and Avitzur [5] modeled extrusion

*Corresponding author. Tel.: +98 833 4274530; Fax: +98 833 4274542.
E-mail address: *hhaghighat@razi.ac.ir* (H. Haghighat).

process through conical die using the upper bound method, but with generalized shear boundaries. Chen and Ling [6] developed a velocity field for axisymmetric extrusion through cosine, elliptic and hyperbolic dies. Nagpal [7] proposed a generalized velocity field in which the deformation region could be optimized. Yang et al. [8] and Yang and Han [9] developed upper bound models with streamlined dies. Osakada and Niimi suggested a generalized expression for the radial flow field for extrusion through a conical die [10]. The shear boundaries have been assumed as two similar curved surfaces. In the study of Peng [11] for extrusion through a conical die, the boundary at the exit of the deformation zone assumed to be a spherical surface with its centre at the apex of cone of the die, and the boundary at the entrance was assumed to be an arbitrarily curved surface. Gordon et al. were analysed extrusion process through spherical dies by upper bound method assuming spherical surfaces for shear boundaries [12]. They were also developed the adaptable die design method for axisymmetric extrusion. The fixed velocity fields were modified by an additional term comprised to two functions. One function allows extra flexibility in the radial direction, and the second function allows extra flexibility in the angular direction. These flexible velocity fields were used in upper bound models for extrusion through dies of any shape. The proposed method by Gordon et al. was described in details in a series of papers [13-15].

As mentioned above, most of research works were focused on the conical die shapes with assuming general shear boundaries or non-conical die shapes with assuming spherical surfaces for shear boundaries. The flow field with spherical boundaries has been used because of simplicity. However, it is known that a field with spherical boundaries gives a higher upper bound value of the extrusion pressure than some other fields for large die angles in conical dies.

In this paper, a generalized expression for the velocity field in axisymmetric extrusion process is suggested that is valid for different dies and the shear boundary shapes of the deformation zone. The boundaries of the deformation zone are assumed to be exponential surfaces and an upper bound solution for extrusion pressure for a rigid-perfectly plastic material is given. The equations are numerically integrated and the solution is optimized by successive approximations with respect to the shape of the zone of plastic deformation to obtain the lowest upper bound value of the extrusion force. After the upper bound model has determined the optimal shapes, a finite element code is used to study the extrusion through dies with these optimal shapes. The upper bound extrusion force is compared with the computational result produced by the finite element method.

2 UPPER BOUND ANALYSIS

Based on the upper bound theory, for a rigid-plastic Von-Misses material and amongst all the kinematically admissible velocity fields, the actual one that minimizes the power required for material deformation is expressed as:

$$J^* = \frac{2\sigma_0}{\sqrt{3}} \int_V \sqrt{\frac{1}{2}\dot{\varepsilon}_{ij}\dot{\varepsilon}_{ij}}\, dV + \int_{S_v} k\,|\Delta v|\, dS + m\int_{S_f} k\,|\Delta v|\, dS - \int_{S_t} T_i v_i\, dS \tag{1}$$

where σ_0 is flow stress of the material, k the material yield strength in shear, $\dot{\varepsilon}_{ij}$ the strain rate tensor, m the constant friction factor, V the volume of plastic deformation zone, S_v and S_f the area of velocity discontinuity and frictional surfaces respectively, S_t the area where the tractions may occur, Δv the amount of velocity discontinuity on the frictional and discontinuity surfaces and v_i and T_i are the velocity and tractions applied on S_t, respectively.

2.1 Geometric description of the deformation zones

Schematic diagram of the axisymmetric extrusion process through an arbitrarily curved die is shown in Fig. 1. In this figure, circular rod with initial radius R_o is extruded through the curved die and its radius is reduced to R_f. A spherical coordinate system (r,θ,φ) is used to describe the velocity in the deformation zones, the die surface and the positions of the two surfaces of velocity discontinuity or shear surfaces. The origin of the spherical coordinate system (r,θ,φ) is located at the intersection of the die axis of symmetry with a line at angle α that goes through the point of die entrance and the exit point of the die. Fig. 1 shows the position of the coordinate system origin. The die surface, which is labeled $\psi(\rho)$ in Fig. 1, is given in the spherical coordinate system. $\psi(\rho)$ is the angular position of

the die surface as a function of the radial distance from the origin. The die length is given by the parameter *L*. The shear boundaries at inlet and outlet of the deformation zone, S_1 and S_2 in Fig. 1, are assumed to be similar arbitrarily $r_o(\beta)$ and $r_f(\beta)$ are geometrically similar, and they are written as a function of angle β as:

$$r_o(\beta) = \rho_o g_o(\beta,\alpha) \tag{2a}$$

$$r_f(\beta) = \rho_f g_o(\beta,\alpha) \tag{2b}$$

and along die surface, it is assumed that

$$r(\theta) = \rho g(\theta,\psi) \tag{2c}$$

where ρ, ρ_o and ρ_f are defined in Fig. 1. The function $g(\beta)$ takes a value of unity at $\beta = \alpha$. For simplicity $g(\beta,\alpha), g(\theta,\psi), r(\theta), r_o(\beta)$ and $r_f(\beta)$ will be abbreviated to g_o, g, r, r_o and r_f, respectively. When the function *g* is equal to 1 the shear boundaries are spherical surfaces and it has no variable parameter and the extrusion pressure is determined uniquely.

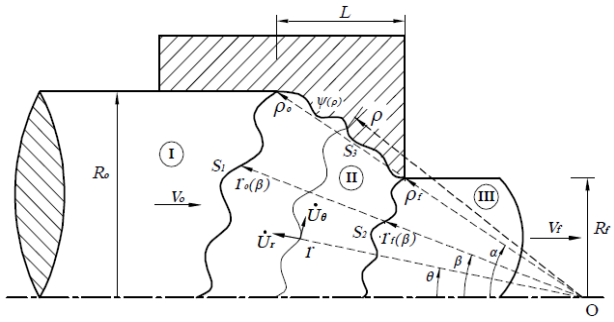

Fig. 1
Schematic diagram of the extrusion process through a curved die, geometric parameters and its deformation zones.

2.2 Velocity fields in different zones

The first step in modelling and analysing a metal forming process by use of upper bound approach is to select a suitable velocity field for the material which is deforming plastically.

In zone I, material does not deform but moves as a rigid body in the axial direction with constant velocity of the punch v_o and we have

$$\dot{U}_r = -v_o \cos\theta, \quad \dot{U}_\theta = v_o \sin\theta, \quad \dot{U}_\varphi = 0 \tag{3}$$

In zone III, the material is already deformed and undergoes no further deformation, moving as a rigid body in the axial direction and the velocity field in spherical coordinate system (r,θ,φ) is

$$\dot{U}_r = -v_f \cos\theta, \quad \dot{U}_\theta = v_f \sin\theta, \quad \dot{U}_\varphi = 0 \tag{4}$$

where v_f is the speed of the extruded rod and from the volume flow balance, we have

$$v_f = \frac{R_o^2}{R_f^2} v_o \tag{5}$$

Zone II is the deformation region and it is bounded by the surface of the die S_3, the boundary S_1 at the inlet and the boundary S_2 at the outlet, as shown in Fig. 1.

The condition of continuity of flow across the inlet boundary S_1 as illustrated in Fig. 2, leads to

$$\tan\lambda = \frac{1}{g_o}\frac{\partial g_o}{\partial \beta} \tag{6}$$

where λ is the angle between direction of the tangent to shear boundary with circumferential direction and angle β is the angular position of a point on surface S_1.

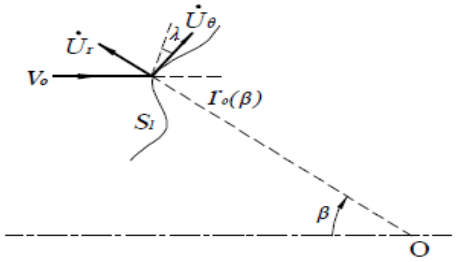

Fig. 2
Velocities at shear surface S_1.

The radial velocity $\dot{U}_{ro}(\beta)$ at the inlet boundary S_1 is

$$\dot{U}_{ro}(\beta) = v_o(\cos\beta + \frac{1}{g_o}\frac{\partial g_o}{\partial \beta}\sin\beta) \tag{7}$$

In Fig. 1, the volume flow of the material across the surfaces S_1 at the point (r_o, β, φ) in the radial direction is

$$dQ = v_o(\cos\beta + \frac{1}{g_o}\frac{\partial g_o}{\partial \beta}\sin\beta)(r_o d\beta)(r_o \sin\beta)d\varphi \tag{8}$$

The volume flow of the material in the radial direction at the point (r, θ, φ) in the deformation zone is

$$dQ = -\dot{U}_r(rd\theta)(r\sin\theta)d\varphi \tag{9}$$

Assuming volume flow balance, the radial velocity $\dot{U}_r$ within the deformation zone can be obtained. Equating Eqs. (8) and (9), the radial velocity component in zone II is found to be

$$\dot{U}_r = -v_o(\frac{r_o}{r})^2\frac{\sin\beta}{\sin\theta}(\cos\beta + \frac{1}{g_o}\frac{\partial g_o}{\partial \beta}\sin\beta)\frac{\partial\beta}{\partial\theta} \tag{10}$$

where v_o is the axial speed of the rod in the entrance of the die.

Assuming proportional distances from die axis of symmetry [13], the relationship between the angular position β on S_1 and the angular position θ in deformation zone II is derived by

$$\frac{\rho_o g_o \sin\beta}{\rho_o \sin\alpha} = \frac{\rho g \sin\theta}{\rho \sin\psi} \tag{11}$$

where angle ψ is the angular position of a point on the die profile at radial position ρ. The equation above is simplified as:

$$\frac{g_o \sin\beta}{\sin\alpha} = \frac{g \sin\theta}{\sin\psi} \tag{12}$$

Differentiating Eq. (12) yields

$$(g_o c\,\mathrm{os}\,\beta + \sin\beta \frac{\partial g_o}{\partial \beta})\frac{\partial \beta}{\partial \theta} = \frac{\sin\alpha}{\sin\psi}(g c\,\mathrm{os}\,\theta + \sin\theta \frac{\partial g}{\partial \theta}) \tag{13}$$

Substituting Eq. (2a) and Eqs. (11)-(13) into Eq. (10), the radial velocity component is simplified as:

$$\dot{U}_r = -v_o (\frac{\rho_o}{r})^2 (\frac{\sin\alpha}{\sin\psi})^2 g^2 (\cos\theta + \frac{1}{g}\frac{\partial g}{\partial \theta}\sin\theta) \tag{14}$$

The full velocity field for the flow of the material in deformation zone II is obtained by invoking volume constancy. Volume constancy in spherical coordinates is defined as:

$$\dot{\varepsilon}_{rr} + \dot{\varepsilon}_{\theta\theta} + \dot{\varepsilon}_{\varphi\varphi} = 0 \tag{15}$$

where $\dot{\varepsilon}_{ii}$ is the normal strain rate component in the i-direction. The strain rates in spherical coordinates are defined as:

$$\begin{aligned}
\dot{\varepsilon}_{rr} &= \frac{\partial \dot{U}_r}{\partial r} \\
\dot{\varepsilon}_{\theta\theta} &= \frac{1}{r}\frac{\partial \dot{U}_\theta}{\partial \theta} + \frac{\dot{U}_r}{r} \\
\dot{\varepsilon}_{\varphi\varphi} &= \frac{1}{r\sin\theta}\frac{\partial \dot{U}_\varphi}{\partial \varphi} + \frac{\dot{U}_r}{r} + \frac{\dot{U}_\theta}{r}\cot\theta \\
\dot{\varepsilon}_{r\theta} &= \frac{1}{2}(\frac{\partial \dot{U}_\theta}{\partial r} - \frac{\dot{U}_\theta}{r} + \frac{1}{r}\frac{\partial \dot{U}_r}{\partial \theta}) \\
\dot{\varepsilon}_{\theta\varphi} &= \frac{1}{2}(\frac{1}{r\sin\theta}\frac{\partial \dot{U}_\theta}{\partial \varphi} + \frac{1}{r}\frac{\partial \dot{U}_\varphi}{\partial \theta} - \frac{\cot\theta}{r}\dot{U}_\varphi) \\
\dot{\varepsilon}_{\varphi r} &= \frac{1}{2}(\frac{\partial \dot{U}_\varphi}{\partial r} - \frac{\dot{U}_\varphi}{r} + \frac{1}{r\sin\theta}\frac{\partial \dot{U}_r}{\partial \varphi})
\end{aligned} \tag{16}$$

where $\dot{\varepsilon}_{ij}$ (with $i \neq j$) is a shear strain rate component. With the assumption of no rotational motion in the deformation zone (i.e. $\dot{U}_\varphi = 0$), a full velocity field is obtained by replacing $\dot{U}_r$, Eq. (14), into Eq. (16) via Eq. (15) and solving for $\dot{U}_\theta$, the angular component of velocity field, then we have

$$\dot{U}_\theta = -v_o \frac{\rho_o^2}{r}(\frac{\sin\alpha}{\sin\psi})^2 \frac{\partial \psi}{\partial r}\frac{1}{\sin\psi} g^2 (\cos\psi - \frac{1}{g}\frac{\partial g}{\partial \psi}\sin\psi)\sin\theta \tag{17}$$

So the total velocity field in deformation zone II is described by

$$\dot{U}_r = -v_o (\frac{\rho_o}{r})^2 (\frac{\sin\alpha}{\sin\psi})^2 g^2 (\cos\theta + \frac{1}{g}\frac{\partial g}{\partial \theta}\sin\theta)$$
$$\dot{U}_\theta = -v_o \frac{\rho_o^2}{r} (\frac{\sin\alpha}{\sin\psi})^2 \frac{\partial\psi}{\partial r}\frac{1}{\sin\psi} g^2 (\cos\psi - \frac{1}{g}\frac{\partial g}{\partial \psi}\sin\psi)\sin\theta \quad (18)$$
$$\dot{U}_\varphi = 0$$

To satisfy boundary condition on die surface; following constraint is applied on function *g* as:

$$\frac{\partial g}{\partial \theta} = -\frac{\partial g}{\partial \psi} \quad at \quad \theta = \psi \quad (19)$$

The Eq. (18) gives the generalized expression for the flow field which includes all the possible die shapes and also boundary shapes of the zone of plastic deformation. A number of velocity fields of flow through conical and curved dies are special cases of the present velocity field. When shear boundaries are assumed as spherical surfaces (i.e. $g = 1$), Eq. (18) each reduce to the velocity field proposed by Gordon et al. [12] for flow through an arbitrarily curved die. When the die shape reduces to a conical die and shear boundaries are assumed as spherical surfaces (i.e. $\psi(r) = \alpha, g = 1$), Eq. (18) each reduce to the spherical velocity field proposed by Avitzur for flow through a conical die [16].With the velocity field, the strain rates in the deformation zone can be given in usual matter. Appendix A gives the six relationships to determine the strain rates components. With the strain rate field and the velocity field, the standard upper bound method can be implemented. This upper bound method involves calculating the internal power of deformation over the deformation zone volume, calculating the shear power losses over the shear surfaces, and the frictional power loss between the material and the die.

2.3 Internal power of deformation

The internal power of deformation is given by

$$\dot{W}_i = \frac{2}{\sqrt{3}}\sigma_0 \int_V \sqrt{\frac{1}{2}\dot{\varepsilon}_{ij}\dot{\varepsilon}_{ij}}\, dV \quad (20)$$

where σ_0 is the mean flow stress of the material and dV is a differential volume in the deformation zone. Internal powers of zones I, III are zero and the general equation to calculate the internal power of deformation in zone II is calculated as:

$$\dot{W}_i = \frac{4\pi}{\sqrt{3}}\sigma_o \int_{\rho_f}^{\rho_o}\int_0^{\psi} \sqrt{\frac{1}{2}\dot{\varepsilon}_{rr}^2 + \frac{1}{2}\dot{\varepsilon}_{\theta\theta}^2 + \frac{1}{2}\dot{\varepsilon}_{\phi\phi}^2 + \dot{\varepsilon}_{r\theta}^2}\ (r\sin\theta) r\, d\theta\, dr \quad (21)$$

where σ_0 is flow stress of material.

2.4 Shear power dissipation

In upper bound method (which includes surfaces of velocity discontinuity), the integration of the shear strength of the material times the tangential velocity difference along the specified surface yields a finite quantity of power. The power loss along a shear surface of velocity discontinuity is given by

$$\dot{W}_S = \frac{\sigma_0}{\sqrt{3}}\int_{S_v} |\Delta v|\, dS \quad (22)$$

Velocities at inlet boundary are shown in Fig. 2. The magnitude of the velocity discontinuity across shear surface S_1 can be written as:

$$\left|\Delta v_1\right| = \left|\dot{U}_r \sin\lambda + \dot{U}_\theta \cos\lambda - v_o \sin(\beta - \lambda)\right| \tag{23}$$

where

$$\sin\lambda = \frac{\frac{1}{g_o}\frac{\partial g_o}{\partial \beta}}{\sqrt{1+(\frac{1}{g_o}\frac{\partial g_o}{\partial \beta})^2}}, \quad \cos\lambda = \frac{1}{\sqrt{1+(\frac{1}{g_o}\frac{\partial g_o}{\partial \beta})^2}} \tag{24}$$

An element of the surface area is

$$dS_1 = 2\pi(r_o \sin\beta) r_o \sqrt{1+(\frac{1}{g_o}\frac{\partial g_o}{\partial \beta})^2}\, d\beta \tag{25}$$

For velocity discontinuity surface S_2

$$\left|\Delta v_2\right| = \left|\dot{U}_r \sin\lambda + \dot{U}_\theta \cos\lambda - v_f \sin(\beta - \lambda)\right| \tag{26}$$

with

$$dS_2 = 2\pi(r_f \sin\beta) r_f \sqrt{1+(\frac{1}{g_o}\frac{\partial g_o}{\partial \beta})^2}\, d\beta \tag{27}$$

Inserting Eqs. (23)-(25) and Eqs. (26)-(27) into Eq. (22), the power dissipated on the velocity discontinuity surfaces S_1 and S_2 are determined as:

$$\dot{W}_{S_1} = \frac{2\pi}{\sqrt{3}}\sigma_o \rho_o^2 \int_0^\alpha \left|\Delta v_1\right| g_o^2 \sqrt{1+(\frac{1}{g_o}\frac{\partial g_o}{\partial \beta})^2}\, \sin\beta\, d\beta \tag{28}$$

$$\dot{W}_{S_2} = \frac{2\pi}{\sqrt{3}}\sigma_o \rho_f^2 \int_0^\alpha \left|\Delta v_2\right| g_o^2 \sqrt{1+(\frac{1}{g_o}\frac{\partial g_o}{\partial \beta})^2}\, \sin\beta\, d\beta \tag{29}$$

2.5 Frictional power dissipation

The general equation for the frictional power loss along a surface with a constant friction factor *m* is

$$\dot{W}_f = m\frac{\sigma_0}{\sqrt{3}}\int_{S_f} \left|\Delta v\right| dS \tag{30}$$

For frictional surface S_3 :

$$\left|\Delta v_3\right| = \left|\dot{U}_r \cos\eta + \dot{U}_\theta \sin\eta\right|_{\theta=\psi} \tag{31}$$

where

$$\cos\eta = \frac{1}{\sqrt{1+(\rho\frac{\partial\psi}{\partial\rho})^2}}, \quad \sin\eta = \frac{\rho\frac{\partial\psi}{\partial\rho}}{\sqrt{1+(\rho\frac{\partial\psi}{\partial\rho})^2}} \tag{32}$$

And

$$dS_3 = 2\pi(\rho\sin\psi)\sqrt{1+(\rho\frac{\partial\psi}{\partial\rho})^2}\,dr \tag{33}$$

Inserting Eqs. (31)-(33) into Eq. (30), gives the frictional power losses along the surface of the die as:

$$\dot{W}_f = \frac{2\pi}{\sqrt{3}} m\sigma_0 \int_{\rho_f}^{\rho_o} |\Delta v_3|(\rho\sin\psi)\sqrt{1+(\rho\frac{\partial\psi}{\partial\rho})^2}\,d\rho \tag{34}$$

where m is the constant friction factor between the material and the die.

The effect of friction in the container is neglected in this study. Therefore, the frictional power loss along the container surface is vanished.

2.6 Total power

Based on the upper bound model, the total power needed for axisymmetric extrusion can be obtained by summing up the internal powers and the powers dissipated on all frictional and velocity discontinuity surfaces as:

$$J^* = \dot{W}_i + \dot{W}_{S1} + \dot{W}_{S2} + \dot{W}_f \tag{35}$$

The externally supplied power, J^*, for axisymmetric extrusion is

$$J^* = P_{ave}\pi R_o^2 v_o \tag{36}$$

Therefore, the total upper bound solution for relative extrusion pressure is given by

$$\frac{P_{ave}}{\sigma_0} = \frac{\dot{W}_i + \dot{W}_{S1} + \dot{W}_{S2} + \dot{W}_f}{\pi R_o^2 v_o \sigma_0} \tag{37}$$

The relative average pressure required for axisymmetric extrusion becomes a function of the process parameters (radii of initial billet and final product, friction factor and die shape) and the parameter associated with the velocity field. Eq. (37) is solved by using a numerical integration method. The solution is optimized by successive approximations with respect to the shape of the zone of plastic deformation. Thus, the lowest upper bound value of the relative extrusion pressure and the die shape with minimum pressure is obtained among its family of boundary shapes.

3 RESULTS AND DISCUSSION

In the theory developed above, different arbitrary boundary function for the plastic deformation zone and dies of different shapes can be employed if the die profile and boundary functions are expressed as equations $\psi(r)$ and

$g(\theta,\psi)$, respectively. The die shape of Yang and Han [10] is examined in the present investigation. They created a streamlined die shape as a fourth-order polynomial whose slope is parallel to the axis at both entrance and exit. Velocity discontinuities do not exist on the inlet and outlet shear boundaries in yang and Han die shape. Therefore, the power of shear deformation consumed on these boundaries vanishes. The equation describing the die shape of Yang and Han in spherical coordinate system (r,θ,φ) was expressed by Ref. [15] as:

$$\frac{\rho}{\rho_o}\frac{\sin\psi}{\sin\alpha}=1+[\frac{C_f}{(1-C_R)^2}-\frac{3}{1-C_R}](-\frac{\rho}{\rho_o}\frac{\cos\psi}{\cos\alpha}+1)^2+[\frac{2}{(1-C_R)^2}-\frac{2C_f}{(1-C_R)^3}](-\frac{\rho}{\rho_o}\frac{\cos\psi}{\cos\alpha}+1)^3+\frac{C_f}{(1-C_R)^4}[-\frac{\rho}{\rho_o}\frac{\cos\psi}{\cos\alpha}+1]^4 \tag{38}$$

with

$$C_f=\frac{3(1-C_R)^2(1-2L_f/L)}{1-6L_f/L+6(L_f/L)^2}\quad,\quad C_R=\frac{\rho_f}{\rho_o} \tag{39}$$

where L_f/L is the position of the inflection point for the die and can vary from 0 to 1and L denotes die length.

In computation, both shear boundaries of S_1 and S_2 are assumed to be portions of similar exponential surfaces whose axes are perpendicular to the axis of the die and pass through the origin O. Surfaces S_1 and S_2 are represented mathematically by equations

$$r_o(\beta)=\rho_o\exp[c\sin\alpha(\frac{\sin\beta}{\sin\alpha}-1)] \tag{40}$$

$$r_f(\beta)=\rho_f\exp[c\sin\alpha(\frac{\sin\beta}{\sin\alpha}-1)] \tag{41}$$

Quantity "c" is a geometric parameter of the shape of the boundary at the inlet and outlet of the deformation zone and can assume negative, zero or positive values. When "c" is negative, the boundaries move away from the origin O, when "c" is positive the boundaries move towards the origin O, when "c" is equal to zero, the boundaries are spherical surfaces and in this case, Eq. (37) has no variable parameter and the extrusion pressure is determined uniquely.Generalized form of the function $g(\theta,\psi)$ and the first derivatives are

$$g(\theta,\psi)=\exp[c\sin\alpha(\frac{\sin\theta}{\sin\psi}-1)] \tag{42}$$

$$\frac{\partial g}{\partial\theta}=c\frac{\sin\alpha}{\sin\psi}\cos\theta\, g\quad,\quad\frac{\partial g}{\partial\psi}=-c\frac{\sin\alpha}{\sin\psi}\frac{\sin\theta}{\sin\psi}\cos\psi\, g \tag{43}$$

It can be seen that $\frac{\partial g}{\partial\theta}=-\frac{\partial g}{\partial\psi}$ at die surface for $\theta=\psi$.

The two combinations of friction factors, initial and final radii of billet are adopted during the analytical solution and the FEM simulation as:

(A) m =0.2, R_o =20 mm and R_f =15 mm

(B) m =0.5, R_o =20 mm and R_f =15 mm

The relative extrusion pressure as a function of "c" for Case A and die length 20 mm is plotted in Fig. 3. The value of "c" at which the relative extrusion pressure is a minimum, represents the assumed boundaries of the plastic zone during actual flow.

Die length has a great influence on the extrusion force. In Fig. 4, comparison between the theoretical extrusion force values versus die length for Cases A and B assuming exponential, Eqs. (40) and (41), and spherical shear boundaries is shown. The calculations have been carried out for a perfectly plastic material with flow stress 200 MPa. It is observed that, for each case there is an optimal die length, which minimizes the extrusion force. It is seen that assuming exponential boundaries for deformation zone yields a better upper bound value of the extrusion force compared to the extrusion force in case of spherical shape boundaries, which is in agreement with the results obtained by the finite element method. This figure also shows that an increase in the friction factor tends to increase the extrusion force.

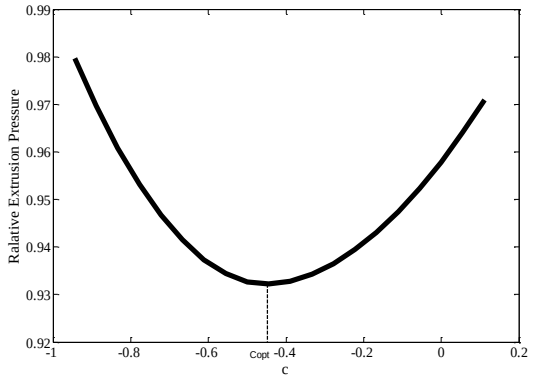

Fig. 3
Variation of relative extrusion pressure with "c" for case A and die length 20 mm.

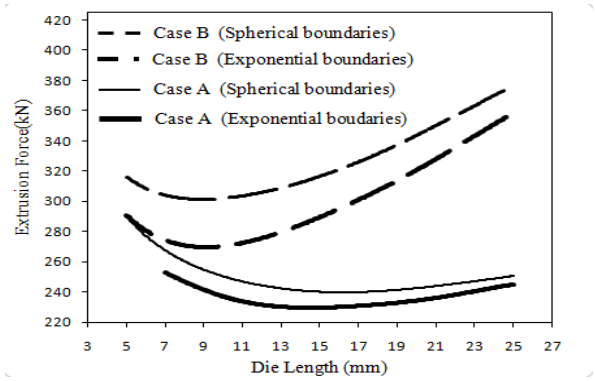

Fig. 4
Comparison between the theoretical extrusion force values versus die length assuming spherical and exponential functions for shear boundaries.

Force in case of spherical shape boundaries is in agreement with the results obtained by the finite element method. This figure also shows that an increase in the friction factor tends to increase the extrusion force.

Optimal die geometries assuming exponential functions for shear boundaries for Cases A and B are shown in Fig. 5. It is seen that the optimal die length becomes shorter with increasing friction factor.

For each optimal die shape, an FEM analysis using ABAQUS is performed to provide results for comparison with the upper bound results. Considering the symmetry in geometry, two-dimensional axisymmetric models are used for FEM analyses. The type of the element used in the model is CAX4R. Punch and container undergo elastic strains only. Thus, it is not necessary to use a fine mesh in these two pieces. However, sufficiently fine meshing is essential deformed material which undergoes plastic deformation. The container is fixed by applying displacement constraint on its nodes while the punch model is loaded by specifying displacement in the axial direction. Fig.6(a) illustrates the mesh used to analyze the deformation. Fig. 6(b) shows the geometry of the deformed mesh for Case A.

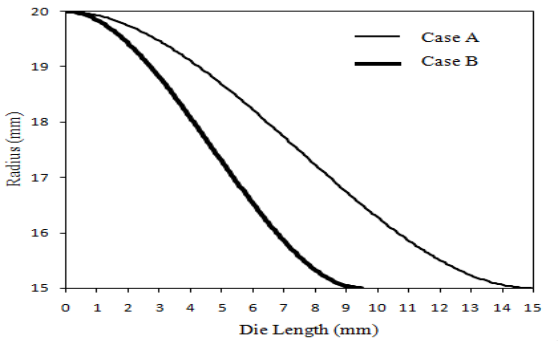

Fig. 5
Optimal die geometries assuming exponential functions for shear boundaries.

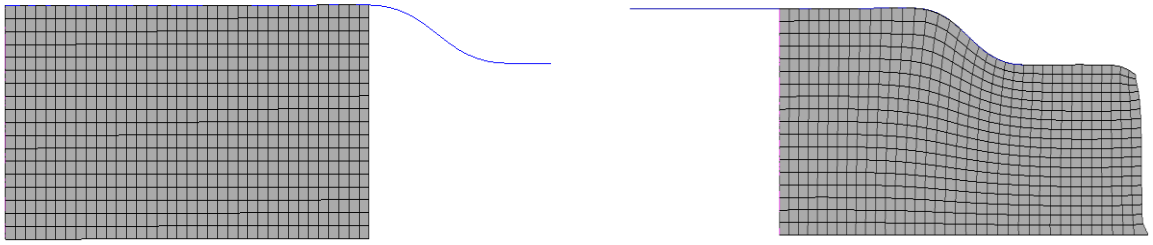

(a) (b)

Fig.6
(a) The finite element mesh, (b) the deformed mesh for Case A.

The most common means of comparing upper bound and FEM results is through extrusion force. Values for the extrusion forces are evaluated from the FEM results. In Fig. 7, FEM force-displacement curves for optimal die shapes are compared. As shown in Fig.7, at the early stage of extrusion, unsteady state deformation occurs, and the materials have not yet filled up the cavity of the die completely. Thus, the extrusion force increases as the extrusion process proceeds. After the materials have filled up the cavity of the die completely, the extrusion force is constant. Because of large non-linearity of the plastic deformation processes, extrusion force curves obtained from ABAQUS have fluctuations as illustrated in Fig. 7. It is seen that assuming exponential boundaries for deformation zone yields a die shape with smaller extrusion force than that of die shape of given by assuming spherical shape boundaries, which is in agreement with the results obtained by the upper bound method. As expected, the predicted extrusion forces are greater than the FEM results, because the present theoretical values are upper bound solutions.

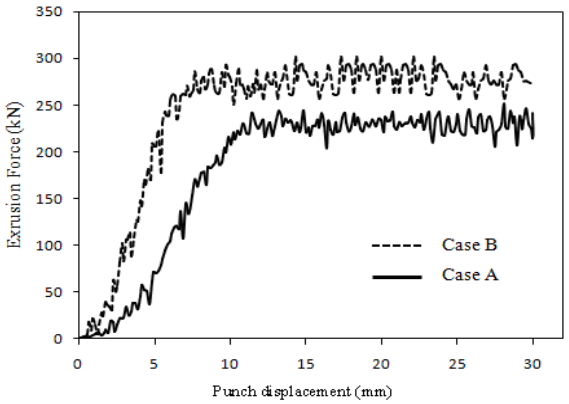

Fig. 7
Comparison of FEM force-displacement curves for optimal die shapes assuming exponential functions for shear boundaries.

4 CONCLUSIONS

In this research, an upper bound model for analysis of the rod extrusion process through arbitrarily curved dies was developed and it was concluded that assuming exponential boundaries for deformation zone yields a better upper

bound value of the extrusion force compared to the extrusion force in case of spherical shape boundaries is in agreement with the results obtained by the finite element method. For a given extrusion conditions, there was an optimal die length which minimizes the extrusion force.With increasing friction factor, the extrusion force increases and the optimal die length becomes shorter.

APPENDIX A

The six relationships to determine the strain rates components are

$$\dot{\varepsilon}_{rr} = v_o (\frac{\rho_o}{r})^2 (\frac{\sin\alpha}{\sin\psi})^2 g^2 [2(\frac{1}{r} + \frac{\partial\psi}{\partial r}\frac{1}{\tan\psi} - \frac{1}{g}\frac{\partial g}{\partial r})(\cos\theta + \frac{1}{g}\frac{\partial g}{\partial\theta}\sin\theta) + (\frac{1}{g^2}\frac{\partial g}{\partial r}\frac{\partial g}{\partial\theta} - \frac{1}{g}\frac{\partial^2 g}{\partial r\partial\theta})\sin\theta] \tag{A.1}$$

$$\dot{\varepsilon}_{\theta\theta} = -v_o (\frac{\rho_o}{r})^2 (\frac{\sin\alpha}{\sin\psi})^2 g^2 [(\cos\theta + \frac{1}{g}\frac{\partial g}{\partial\theta}\sin\theta)\frac{1}{r} + \frac{\partial\psi}{\partial r}\frac{1}{\sin\psi}(\cos\psi - \frac{1}{g}\frac{\partial g}{\partial\psi}\sin\psi)\cos\theta + \frac{\partial\psi}{\partial r}\frac{1}{\sin\psi}\frac{\partial g}{\partial\theta}\frac{2}{g}(\cos\psi - \frac{1}{g}\frac{\partial g}{\partial\psi}\sin\psi)\sin\theta + \frac{\partial\psi}{\partial r}(\frac{1}{g^2}\frac{\partial g}{\partial\theta}\frac{\partial g}{\partial\psi} - \frac{1}{g}\frac{\partial^2 g}{\partial\theta\partial\psi})\cos\theta] \tag{A.2}$$

$$\dot{\varepsilon}_{\varphi\varphi} = -v_o \frac{\rho_o^2}{r^3}(\frac{\sin\alpha}{\sin\psi})^2 g^2 [(\cos\theta + \frac{1}{g}\frac{\partial g}{\partial\theta}\sin\theta) + \frac{\partial\psi}{\partial r}\frac{1}{\sin\psi}(\cos\psi - \frac{1}{g}\frac{\partial g}{\partial\psi}\sin\psi)\cos\theta] \tag{A.3}$$

$$\dot{\varepsilon}_{r\theta} = \frac{v_o}{2}(\frac{\rho_o}{r})^2 (\frac{\sin\alpha}{\sin\psi})^2 \{2g^2\frac{\partial\psi}{\partial r}\frac{\sin\theta}{\sin\psi} - g\frac{\partial g}{\partial r}\sin\theta + 2rg(\frac{\partial\psi}{\partial r})^2\frac{\sin\theta}{\tan^2\psi} - 4rg\frac{\partial\psi}{\partial r}\frac{\partial g}{\partial r}\frac{\sin\theta}{\tan\psi} - rg^2\frac{\partial^2\psi}{\partial r^2}\frac{\sin\theta}{\tan\psi} + r(\frac{\partial\psi}{\partial r})^2\frac{1}{\sin^2\psi}\sin\theta + rg\frac{\partial^2 g}{\partial r^2}\sin\theta + r(\frac{\partial g}{\partial r})^2\sin\theta - g\frac{\partial g}{\partial r}\sin\theta - (2g + \frac{1}{g})\frac{\partial g}{\partial\theta}\frac{\cos\theta}{r} - [(\frac{\partial g}{\partial\theta})^2 + g\frac{\partial^2 g}{\partial\theta^2} - g^2]\frac{\sin\theta}{r}\} \tag{A.4}$$

$$\dot{\varepsilon}_{\theta\varphi} = 0 \tag{A.5}$$

$$\dot{\varepsilon}_{\varphi r} = 0 \tag{A.6}$$

where

$$\frac{\partial\psi}{\partial r} = \frac{\partial\psi}{\partial\rho}\frac{\partial\rho}{\partial r} \tag{A.7}$$

$$\frac{\partial\rho}{\partial r} = \frac{1}{g + \rho\frac{\partial g}{\partial\psi}\frac{\partial\psi}{\partial\rho}} \tag{A.8}$$

and

$$\frac{\partial g}{\partial r} = \frac{\partial g}{\partial\psi}\frac{\partial\psi}{\partial r} \tag{A.9}$$

REFERENCES

[1] Avitzur B., 1963, Analysis of wire drawing and extrusion through conical dies of small cone angle, *Transactions of the ASME, Journal of Engineering for Industry* **85**: 89-96.

[2] Avitzur B., 1964, Analysis of wire drawing and extrusion through conical dies of large cone angle, *Transactions of the ASME, Journal of Engineering for Industry* **86**: 305-314.

[3] Avitzur B., 1966, Flow characteristics through conical converging dies, *Transactions of the ASME, Journal of Engineering for Industry* **88**: 410-420.

[4] Avitzur B., 1967, Strain-hardening and strain-rate effects in plastic flow through conical converging dies, *Transactions of the ASME, Journal of Engineering for Industry* **89**: 556-562.

[5] Zimerman Z., Avitzur B., 1970, Metal flow through conical converging dies-a lower upper bound approach using generalized boundaries of the plastic zone, *Transactions of the ASME, Journal of Engineering for Industry* **92**: 119-129.

[6] Chen C. T., Ling F. F., 1968, Upper bound solutions to axisymmetric extrusion problems, *International Journal of Mechanical Sciences* **10**: 863-879.

[7] Nagpal V., 1974, General kinematically admissible velocity fields for some axisymmetric metal forming problems, *Transactions of the ASME, Journal of Engineering for Industry* **96**: 1197-1201.

[8] Yang DY D.Y., Han CH C.H., Lee B.C., 1985, The use of generalised deformation boundaries for the analysis of axisymmetric extrusion through curved dies, *International Journal of Mechanical Sciences* **27**: 653-663.

[9] Osakada K., Niimi Y., 1975, A study on radial flow field for extrusion through conical dies, *International Journal of Mechanical Sciences* **17**: 241-254.

[10] Yang D. Y., Han C. H., 1987, A new formulation of generalized velocity field for axisymmetric forward extrusion through arbitrarily curved dies, *Transactions of the ASME, Journal of Engineering for Industry* **109**: 161-168.

[11] Peng D. S., 1990, An upper bound analysis of the geometric shape of the deformation zone in rod extrusion, *Journal of Materials Processing Technology* **21**: 303-311.

[12] Gordon W. A., Van Tyne C. J., Sriram S., 2002, Extrusion through spherical dies—an upper bound analysis, *Transactions of the ASME,Journal of Manufacturing Science and Engineering* **124**: 92-97.

[13] Gordon W. A., Van Tyne C. J., Moon Y. H., 2007, Axisymmetric extrusion through adaptable dies—Part 1: Flexible velocity fields and power terms, *International Journal of Mechanical Sciences* **49**: 86-95.

[14] Gordon W. A., Van Tyne C. J., Moon Y. H., 2007, Axisymmetric extrusion through adaptable dies—Part 2: Comparison of velocity fields, *International Journal of Mechanical Sciences* **49**: 96-103.

[15] Gordon W. A., Van Tyne C. J., Moon Y. H., 2007, Axisymmetric extrusion through adaptable dies—Part 3: Minimum pressure streamlined die shapes, *International Journal of Mechanical Sciences* **49**: 104-115.

[16] Avitzur B., 1968, *Metal Forming: Processes and Analysis*, New York, NY: McGraw-Hill.